

Propranolol Activates the Orphan Nuclear Receptor TLX to Counteract Proliferation and Migration of Glioblastoma Cells

Giuseppe Faudone, Iris Bischoff-Kont, Lea Rachor, Sabine Willems, Rezart Zhubi, Astrid Kaiser, Apirat Chaikuad, Stefan Knapp, Robert Fürst, Jan Heering, and Daniel Merk*

Cite This: *J. Med. Chem.* 2021, 64, 8727–8738

Read Online

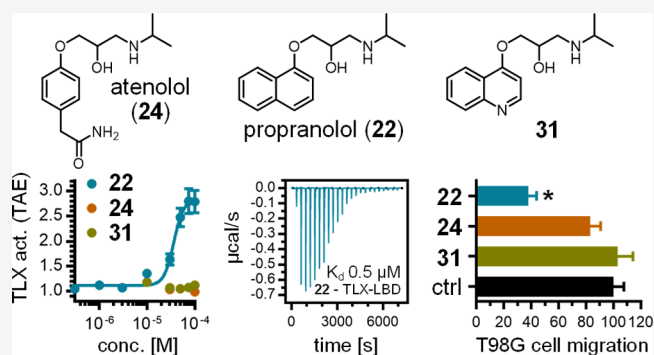
ACCESS |

Metrics & More

Article Recommendations

Supporting Information

ABSTRACT: The ligand-sensing transcription factor tailless homologue (TLX, NR2E1) is an essential regulator of neuronal stem cell homeostasis with appealing therapeutic potential in neurodegenerative diseases and central nervous system tumors. However, knowledge on TLX ligands is scarce, providing an obstacle to target validation and medicinal chemistry. To discover TLX ligands, we have profiled a drug fragment collection for TLX modulation and identified several structurally diverse agonists and inverse agonists of the nuclear receptor. Propranolol evolved as the strongest TLX agonist and promoted TLX-regulated gene expression in human glioblastoma cells. Structure–activity relationship elucidation of propranolol as a TLX ligand yielded a structurally related negative control compound. In functional cellular experiments, we observed an ability of propranolol to counteract glioblastoma cell proliferation and migration, while the negative control had no effect. Our results provide a collection of TLX modulators as initial chemical tools and set of lead compounds and support therapeutic potential of TLX modulation in glioblastoma.



INTRODUCTION

The tailless homologue TLX (NR2E1) is an orphan member of the protein family of nuclear receptors (NRs), which act as ligand-dependent transcriptional regulators. In adults, TLX expression is strongly limited and only found in neural stem cells (NSCs) and retinal progenitor cells.^{1,2} Current evidence suggests that TLX mainly acts as a transcriptional repressor that recruits histone deacetylases, lysine-specific histone demethylase-1, REST corepressor 1, atrophin-1, and oncoprotein B-cell lymphoma 11A to suppress the expression of tumor suppressors such as p21 and the phosphatase and tensin homologue (PTEN).^{3–6} However, there are also genes that are positively regulated by TLX activity such as sirtuin 1 (SIRT1).⁷ Observations from animal models characterize TLX as an essential factor to maintain NSCs in an undifferentiated, proliferating state.⁸ TLX mutations were found to disturb neurogenesis, and TLX knockout triggered an aggressive behavior and abnormal brain development.^{8–10} In human patients, mutations or altered expression of TLX is associated with mental disorders, and the receptor is attributable for important functions in cognitive function and learning.^{11–14} Based on these observations, TLX agonists may present great therapeutic potential in neurodegenerative and neurological disorders, but pharmacological validation of this hypothesis remains elusive. In addition to the crucial involvement of TLX in neuronal homeostasis, altered TLX expression was detected

in glioblastoma and neuroblastoma cells.^{15,16} This suggests that TLX plays a role in brain tumor development and progression and might also hold therapeutic potential in this regard.

Despite the remarkable promise of the orphan NR TLX as a potential target for the treatment of neurodegeneration and central nervous system (CNS) tumors, only a few weak TLX ligands have been discovered to date.^{17–19} TLX modulators to serve as pharmacological tools for target validation of TLX are lacking.

To expand the sparse knowledge on TLX ligand chemotypes and discover tools to study TLX biology, we have systematically profiled a collection of 480 drug fragments for TLX modulation *in vitro*. We identified several structurally diverse TLX modulator scaffolds including activators and inverse agonists presenting as early tools and as attractive starting points for medicinal chemistry. Subsequent expansion to the related drug molecules revealed several TLX modulating drugs, among which propranolol (22) acted as the strongest agonist activating TLX in several orthogonal cellular settings. Binding

Received: April 23, 2021

Published: June 11, 2021



of propranolol (**22**) to the TLX ligand-binding domain (LBD) with sub-micromolar affinity was confirmed by isothermal titration calorimetry (ITC). Through systematic structural variation of the β adrenoceptor blocker, we have elucidated the structure–activity relationship (SAR) of propranolol (**22**) as TLX activator and identified a close structural analogue lacking activity on TLX, which can serve as a valuable negative control. Intriguingly, treatment of human glioblastoma cells with propranolol (**22**) decreased their proliferation and migration, while the negative control had no effect. Our results provide important insights into modulation of the orphan receptor TLX and characterize propranolol (**22**) as a useful early tool equipped with a negative control for functional studies.

RESULTS AND DISCUSSION

We used a cellular reporter gene assay to discover chemical starting matter for TLX modulator development. Since TLX acts as a transcriptional repressor,^{3–6} we established a cellular reporter gene assay, capturing this peculiar characteristic as a screening system. It relies on the Gal4 hybrid technique²⁰ and incorporates the ligand-independent transcriptional activator Gal4-VP16^{21,22} to induce reporter (firefly luciferase) activity, which is countered by Gal4-TLX (composed of the Gal4 DNA-binding domain and the human TLX LBD). The assay conditions were optimized to allow observation of bidirectional TLX modulation including TLX activation and inverse TLX agonism (see Figure S1). In addition, this setting enabled an important control experiment by verifying the effect of test compounds modulating Gal4-VP16/Gal4-TLX on Gal4-VP16 alone. Using this TLX reporter gene assay, we screened the core set of the Prestwick Drug-Fragment Library, a collection of 480 common fragment structures of FDA-approved drugs, which comprises a chemically diverse set of fragment structures with favorable properties complying with the rule of 3 (see ref 23 for features and all contained fragments). Despite containing no steroidal elements, this fragment library has revealed novel NR ligands in previous applications.²³ The entire fragment library was screened at 100 μ M in two independent repeats, and fragments inducing a reporter activity ≤ 0.5 -fold (TLX agonists) or ≥ 1.5 -fold (inverse TLX agonists) compared to that of dimethylsulfoxide (DMSO)-treated cells were considered as primary hits. After curation for test compound toxicity (observed by effects on constitutive *Renilla* luciferase activity) and pan-assay interference substances (PAINS), 20 fragments (**1–20**) were considered as primary hits (Tables 1 and S1), of which 14 scaffolds were retained after control experiments on Gal4-VP16 to reveal non-specific activity (Table 1).

However, NR activity can also be regulated indirectly involving, for example, altered expression levels, post-translational modifications, and complex monomer–oligomer equilibria.²⁴ Accordingly, indirect NR modulators have been reported, for example, for Nur77^{25,26} and HNF4 α .²³ Hence, we used a secondary cellular screening system based on a reporter construct for human full-length TLX with the TLX-activated element (TAE)⁷ from the SIRT1 promoter region to control reporter expression for further validation. This TAE assay was performed in HEK293T cells, and full-length human TLX (fTLX) was overexpressed. In contrast to the Gal4-TLX system in which TLX activators cause increased repression and hence a lower reporter signal, reporter expression under TAE control is induced by TLX agonists (and vice versa for inverse TLX agonists). These two cellular assays detecting opposite

Table 1. Fragment Screening Hits

ID	structure	Gal4-TLX ^a (fold. act.)	TAE ^b (fold. act.)	DSF ^c (ΔT_m [°C])
2		0.47±0.03	2.20±0.06	1.2
4		0.32±0.06	0.68±0.05	1.1
5		0.27±0.08	3.2±0.2	1.5
7		0.47±0.05	1.12±0.06	0.6
8		3.3±0.3	1.47±0.08	1.1
9		0.17±0.07	0.57±0.06	-0.5
10		0.37±0.01	0.57±0.04	-2.3
11		0.34±0.04	0.41±0.02	-1.4
12		0.5±0.2	0.86±0.03	0.8
13		2.7±0.5	1.33±0.08	0.5
16		0.44±0.04	0.65±0.03	-3.2
18		2.9±0.5	1.8±0.2	1.2
19		0.45±0.01	2.1±0.2	2.4
20		0.46±0.02	1.05±0.09	-0.3

^aGal4-TLX + Gal4-VP16 with Gal4-responsive firefly luciferase was used for the primary screen. Data are mean \pm standard deviation (SD) reporter activity of 100 μ M test compound vs DMSO (0.4%)-treated cells, $n = 2$. ^bA TAE luciferase reporter responsive to fTLX was used as secondary screen. Data are mean \pm standard error of the mean (SEM) reporter activity of 100 μ M test compound vs DMSO (0.1%)-treated cells, $n = 3$. ^cDSF with recombinant TLX-LBD served as a cell-free counter-screen. Data are mean ΔT_m at 500 μ M compound, $N = 3$.

effects of TLX ligands on reporter activity therefore complemented each other (Figure S1). Additionally, we performed differential scanning fluorimetry (DSF) using recombinant human TLX-LBD as a third cell-free counter-screen. Both secondary and tertiary assays fully confirmed TLX activation and direct interaction for fragments **2**, **5**, and **19**. These TLX agonists promoted the repressor activity of Gal4-TLX and enhanced fTLX activity on the TAE. In addition, **8**, **13**, and **18** were identified as direct TLX modulators causing derepression in the Gal4-TLX assay and fTLX activation on the TAE. All six TLX modulators stabilized the TLX LBD, indicated by positive melting temperature shifts (ΔT_m) of 1.1–

Table 2. Validated Fragment TLX Agonists

ID	structure	Gal4-TLX ^a	TAE ^b
2		EC ₅₀ 74±18 μM (0.4±0.1 remain.)	EC ₅₀ > 100 μM (2.15-fold act. at 100 μM)
5		EC ₅₀ 19.4±0.9 μM (0.07±0.03 remain.)	EC ₅₀ 43±9 μM (2.3±0.3 fold act.)
19		EC ₅₀ 67±8 μM (0.50±0.03 remain.)	EC ₅₀ > 100 μM (1.98-fold act. at 100 μM)

^aGal4-TLX + Gal4-VP16 with Gal4-responsive firefly luciferase. Remaining activity compared to 0.1% DMSO-treated cells. Data are the mean ± SEM, $n \geq 3$. ^bTAE luciferase reporter and fTLX. Fold activation compared to 0.1% DMSO-treated cells. Data are the mean ± SEM, $n = 3$.

2.4 °C in the DSF assay. In line with previous reports,¹⁷ the reference TLX ligands dydrogesterone and ccrp2 destabilized the TLX LBD with thermal shifts of -1.9 and -1.6 °C, respectively.

Full dose–response profiling of the fragment TLX agonists 2, 5, and 19 on Gal4-TLX and fTLX/TAE consistently revealed potencies in the single/double-digit micromolar range (Table 2). These orthogonally validated fragment TLX ligands not only serve as a potential chemical tool to study TLX biology but also present an attractive starting point for the development of potent TLX modulators.

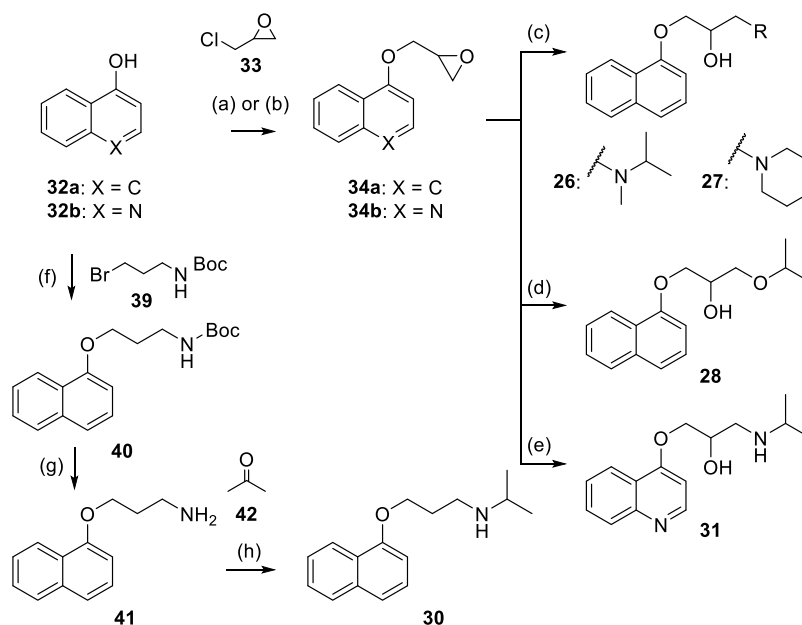
We then followed up on the most active TLX agonists (Table 2) by performing a substructure search in the DrugBank²⁷ for each fragment and evaluated approved drugs associated with the respective fragment structures for TLX modulation in the Gal4-VP16/Gal4-TLX assay (Table 3).

Table 3. Activity of Approved Drugs on TLX^a

drug INN	structure	Gal4-TLX
Tadalafil 21		EC ₅₀ 5±1 μM (0.62±0.04 remain.)
Propranolol rac-22		EC ₅₀ 32±4 μM (0.08±0.08 remain.)
Propafenone rac-23		EC ₅₀ 47±10 μM (0.2±0.1 remain.)
Atenolol rac-24		inactive
Sotalol rac-25		inactive

^aGal4-TLX + Gal4-VP16 with Gal4-responsive firefly luciferase. Structural differences of 21 and 22 to the active fragment structure discovered in the screening in red. Activities were validated against Gal4-VP16. Data are the mean ± SEM; $n \geq 3$. Fold activation or remaining activity refers to the maximum effect on reporter activity relative to DMSO (0.1%)-treated cells.

Tadalafil (21, from fragment 2) and propranolol (22, from fragment 5) were confirmed to be active on TLX. Tadalafil (21) exhibited TLX agonism with an EC₅₀ value of 5 μM but

Scheme 1. Synthesis of 26–28, 30, and 31^a

^aReagents and conditions: (a) Dimethylformamide (DMF)/H₂O, NaOH, room temperature (rt), 120 h, 11%. (b) Acetone, NaH, rt, 48 h, 27%. (c) *N*-Methylisopropylamine (35) or piperidine (36), μ w, 100 °C, 30–45 min, 29–89%. (d) *i*PrOH (37), NaH, rt, 12 h, 90%. (e) *i*PrNH₂ (38), 60 °C, 10 h, HCl–dioxane (4 M), rt, 72 h, 87%. (f) DMF, NaH, rt, 24 h, 88%. (g) Dichloromethane, HCl–dioxane (4 M), rt, 21 h, 80%. (h) 1,2-Dichloroethane, triethylamine, acetic acid, NaB(OAc)₃H, rt, 17 h, 46%.

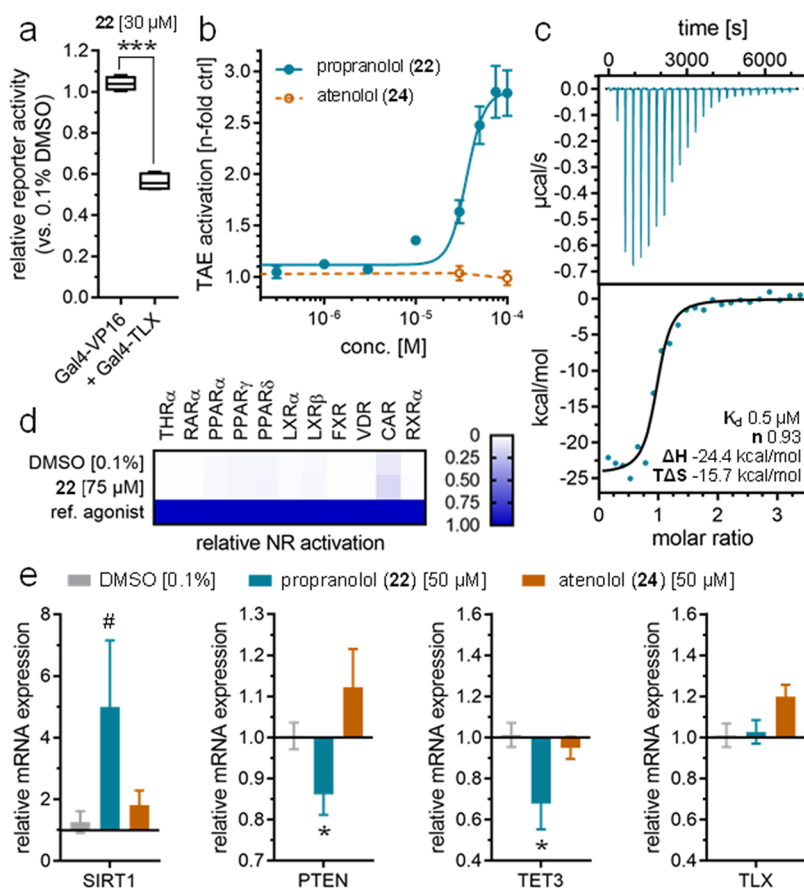
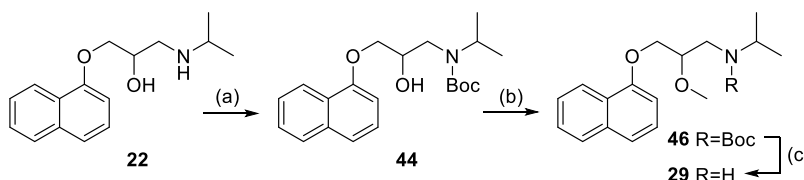


Figure 1. Profiling of propranolol (**22**) as a TLX activator. (a) Control experiments on Gal4-VP16 in the absence of Gal4-TLX revealed no non-specific effect of propranolol (**22**), confirming TLX-mediated activity. The boxplot shows min–max, $n = 4$. *** $p < 0.001$. (b) Propranolol (**22**) activated the TAE with an EC₅₀ value of 37 μM; atenolol (**24**) was inactive. Data are the mean ± SEM, $n \geq 3$. (c) ITC of the propranolol (**22**)–TLX interaction. The isotherm after subtraction of ligand dilution heat is shown in the top panel, and the fitting of the heat of binding is shown below. (d) Propranolol (**22**) was selective in a panel of NRs except weak CAR activation. The heatmap shows mean relative NR activation compared to reference agonists, $n = 3$. (e) Propranolol (**22**) modulated TLX-regulated gene expression in human T98G glioblastoma cells with induction of SIRT1 and downregulation of the PTEN and TET3. The expression level of TLX was not affected by propranolol (**22**), and atenolol (**24**) had no significant effect on SIRT1, PTEN, and TET3 expression. Data are the mean ± SEM, $n = 4$. # $p < 0.1$, * $p < 0.05$.

Scheme 2. Synthesis of **29**^a



^aReagents and conditions: (a) H₂O, Boc₂O (**43**), NaHCO₃, rt, 18 h, quant. (b) DMS (**45**), μw, 60 °C, 3 h, 14%. (c) HCl–1,4-dioxane, rt, 12 h, 90%.

with weak efficacy. Propranolol (**22**), in contrast, enhanced TLX activity with a remarkable efficacy of more than 10-fold (8% remaining VP16-induced reporter activity) and moderate potency (EC₅₀ 32 μM). Importantly, propranolol (**22**) did not affect Gal4-VP16 activity in the absence of Gal4-TLX (Figure 1a).

Intrigued by the marked TLX agonism of propranolol (**22**), we next studied a potential TLX modulation by related β adrenoceptor antagonists. Propafenone (**23**) exhibited considerable TLX activation, while atenolol (**24**) and sotalol (**25**) were inactive. The lack of TLX modulation by the structurally related drugs **24** and **25** additionally validated the activity of propranolol (**22**) as TLX-mediated. To further profile

propranolol (**22**) as a TLX agonist, we probed its activity on fTLX using the TAE reporter. Indeed, propranolol (**22**) robustly induced activity of fTLX on TAE with an EC₅₀ value of 37 μM, while atenolol (**24**) was inactive (Figure 1b). This was additionally supported by ITC, confirming direct propranolol–TLX interaction with a K_d of 0.5 μM (Figure 1c).

When we treated TLX-expressing human glioblastoma cells (T98G) with propranolol (**22**) and quantified messenger RNA (mRNA) levels of TLX-regulated genes, we observed induction of SIRT1⁷ and repression of PTEN³ and the Tet methylcytosine dioxygenase 3 (TET3)²⁸ (Figure 1e). The expression level of TLX was not affected. This indicated therefore that propranolol (**22**) enhanced TLX activity *via*

direct activation. On the contrary, atenolol (**24**) did not alter TLX-regulated gene expression apart from slight upregulation of PTEN, suggesting no effect toward TLX activation.

The pronounced TLX agonism in three orthogonal cellular settings with confirmed direct binding and high selectivity among NRs (Figure 1d) rendered **22** as an attractive chemical tool for biological studies and a starting point for ligand optimization. The different activities of **22–25** already provided first insights into the SAR of propranolol as a TLX activator and suggested the naphthalen system of propranolol (**22**) as a favored motif for TLX activation. To obtain further insights into the SAR of propranolol as a TLX agonist, we studied key pharmacophore elements of the scaffold by systematic structural modifications (**26–31**, Table 4).

Propranolol derivatives **26–31** were prepared according to Schemes 1 and 2. Compounds **26–28** and **31** were prepared over two steps following a published route²⁹ with minor modifications. 1-Naphthol (**32a**) and quinoline-4-ol (**32b**) were reacted with *rac*-epichlorohydrin (**33**) to **34a** and **34b**, respectively. Subsequently, the epoxide in **34a** was opened with *N*-methylisopropylamine (**35**), piperidine (**36**), or isopropanol (**37**), yielding the corresponding alcohols **26–28**. Epoxide **34b** was opened with *iso*-propylamine (**38**), yielding aminoalcohol **31** [Scheme 1, (a–e)]. Analogue **30** lacking the hydroxy group was synthesized by nucleophilic substitution of *tert*-butyl-(3-bromopropyl)carbamate (**39**) with 1-naphthol (**32a**) followed by acidic Boc cleavage to **41** and reductive amination with acetone (**42**) using NaB(OAc)₃H to **30** [Scheme 1, (f–h)].^{30,31} Methoxy analogue **29** was prepared from propranolol (**22**) by Boc protection of the secondary amine to **44** followed by methylation with dimethyl sulfate (**45**, DMS) under microwave irradiation to **46** and Boc cleavage to **29** (Scheme 2).

To capture the SAR of propranolol (**22**) as a TLX activator, we systematically analyzed the contributions of its molecular features to TLX modulation (Table 4). *In vitro* characterization of the two propranolol enantiomers *R*-propranolol (**22a**) and *S*-propranolol (**22b**) revealed no preference for an eutomer. Thus, we continued further SAR studies with racemic compounds and next probed the contribution of the secondary amine motif. *N*-Methylation (**26**) or replacement of the isopropylamine with a bulky piperidine residue (**27**) was detrimental for activity, and the isopropyl ether analogue **28** was less active than **22**, demonstrating the importance of the secondary amine likely as a H-bond donor. Methylation of the secondary hydroxyl group (**29**) or its removal (**30**), in contrast, was accompanied only by a moderate loss in activity. Overall, however, all structural features of the original drug propranolol (**22**) appeared favorable for TLX activation. Following the observation that nitrogen-containing two-ring heterocycles were favored by TLX (fragments **2**, **8**, **18**, and **19**), we prepared the quinoline analogue **31** of propranolol (**22**), which, however, was inactive on TLX up to 300 μ M. The absence of TLX modulation by **31** was also confirmed using the TAE reporter and flTLX. With this lack of activity and its remarkable structural similarity to the TLX agonist **22**, **31** evolved as a useful negative control compound.

TLX has been found to be overexpressed in glioblastoma and neuroblastoma cells, indicating a potential role in CNS tumors,^{15,16} and gene expression analysis of propranolol (**22**)-treated glioblastoma cells (Figure 1d) confirmed effects of TLX activation on TLX-regulated SIRT1, PTEN, and TET3. To reveal a potential phenotypic effect of TLX modulation by

Table 4. Activity of Propranolol Derivatives on TLX^a

ID	structure	Gal4-TLX modulation EC ₅₀ (remain. act.)
5		19±1 μ M (0.07±0.03)
<i>rac</i> - 22		32±4 μ M (0.08±0.08)
<i>R</i> - 22a		40±6 μ M (0.40±0.09)
<i>S</i> - 22b		72±9 μ M (0.25±0.10)
26		>100 μ M
27		inactive (100 μ M)
28		83±14 μ M (0.29±0.15)
29		52±13 μ M (0.28±0.08)
30		50±2 μ M (0.42±0.04)
31		inactive (300 μ M)

^aGal4-TLX + Gal4-VP16 with Gal4-responsive firefly luciferase. Activities were validated against Gal4-VP16. Data are the mean \pm SEM; $n \geq 3$. Remaining activity refers to the maximum repression of reporter activity relative to DMSO (0.1%)-treated cells.

propranolol on brain tumor cells, we treated human glioblastoma cells (T98G) with propranolol (**22**), its inactive analogue **31**, or the β adrenoceptor antagonists **24** and **25** and studied apoptosis, proliferation, and migration (Figure 2). We first analyzed potential cytotoxic effects of the compounds by measuring WST-1 conversion, lactate dehydrogenase (LDH) release, and apoptosis upon treatment of T98G cells with **22**, **24**, **25**, or **31**. Apart from slightly reduced viability at 100 μ M in the WST-1 assay, propranolol (**22**), the β adrenoceptor antagonists **24** and **25**, and the negative control **31** exhibited no toxic or pro-apoptotic effect (Figure 2a–c). In a crystal violet uptake assay (Figure 2d,e), however, propranolol (**22**) revealed pronounced anti-proliferative activity on T98G cells, while **24**, **25**, and **31** were inactive. Moreover, propranolol (**22**) antagonized the migration of T98G cells toward a fetal calf serum (FCS) gradient in a Boyden chamber, while **24**, **25**, and **31** had no effect (Figure 2f).

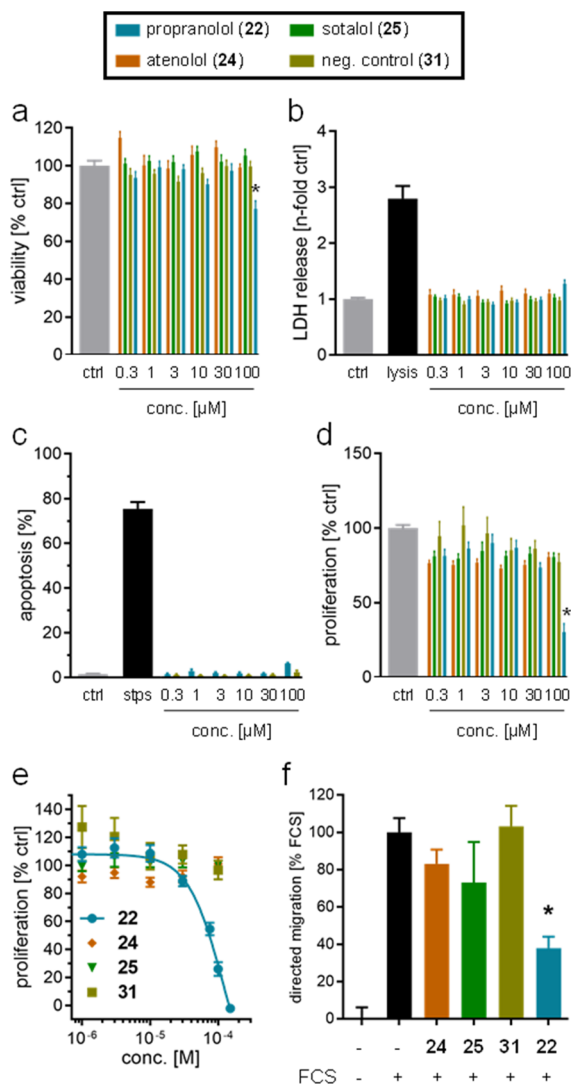


Figure 2. Effects of TLX agonist propranolol (**22**) on human T98G glioblastoma cells. The β adrenoceptor antagonists **24** and **25** and the structural analogue **31** were used as negative control compounds lacking TLX agonism. (a–c) **22**, **24**, **25**, and **31** exhibited no toxic effects on T98G glioblastoma cells as determined by WST-1 conversion (a), LDH release (b), and apoptosis staining with propidium iodide (PI)³² (c). Data are the mean \pm SEM, $n = 3$. stps—staurosporin. (d,e) **22** inhibited the proliferation of T98G glioblastoma cells with an IC_{50} of approx. $75 \mu\text{M}$ as determined by crystal violet uptake. Compounds **24**, **25**, and **31** were inactive. Data are the mean \pm SEM, $n = 3$. (f) **22** ($75 \mu\text{M}$) inhibited migration of T98G glioblastoma cells in an FCS gradient in a Boyden chamber. Compounds **24**, **25**, and **31** ($75 \mu\text{M}$ each) were inactive. Data are the mean \pm SEM, $n = 3$. * $p < 0.05$.

The considerable anti-proliferative and migration-inhibiting effect of the TLX agonist and β adrenoceptor antagonist propranolol (**22**) and the absence of such an effect for the β adrenoceptor antagonists **24** and **25** lacking activity on TLX and the negative propranolol analogue **31** strongly suggest that the effects of propranolol were TLX-mediated. These observations further support an important role of TLX in glioblastoma and indicate therapeutic potential of TLX modulation.

CONCLUSIONS

Several knockout studies and observations from human patients suggest the orphan NR TLX as an essential regulator of NSC maintenance with therapeutic potential as molecular target in neurodegenerative diseases. Moreover, TLX was found to be overexpressed in brain tumors and might, hence, open new avenues in this indication too. However, further evaluation and validation of this therapeutic potential are hindered by the lack of chemical tools to study the roles of TLX in health and disease. To provide rapid access to TLX-modulating small molecules, we have conducted a drug fragment screen, which has yielded a collection of orthogonally validated, structurally diverse TLX ligand chemotypes. This set of TLX modulators can serve as an early chemical tool for pharmacological control of TLX activity and is very valuable as a pool of lead compounds for medicinal chemistry. Propranolol (**22**) evolved as the most effective TLX agonist and activated TLX in three different cellular settings. ITC confirmed the direct interaction of propranolol (**22**) with the TLX LBD with sub-micromolar affinity. Nevertheless, complex structures will be required to provide insights into the binding mode of propranolol (**22**) to TLX.

Treatment of human glioblastoma cells with the TLX agonist propranolol (**22**) caused a pronounced reduction in proliferation and migration. The β adrenoceptor antagonists atenolol (**24**) and sotalolol (**25**) lacking TLX agonism did not affect glioblastoma cells, and the structural analogue **31** was inactive, too, strongly pointing to TLX-mediated effects of propranolol (**22**). This phenotypic effect provides further evidence that TLX plays a role in brain cancer and indicates that TLX modulation can be pharmacologically exploited in this indication.

EXPERIMENTAL SECTION

Chemistry. General. All chemicals and solvents were purchased from commercial sources and used without further purification. Reactions were carried out in absolute solvents. Argon was used as inert gas if required. Reactions were monitored by thin-layer chromatography (TLC) using TLC plates (silica gel 60 F₂₅₄, 0.2 mm, Merck or Alugram Xtra Sil G/UV 0.2 mm, Macherey Nagel) with UV-light ($\lambda = 254$ and 366 nm) detection or using ninhydrin, potassium permanganate, phosphomolybdic acid, or cerium molybdate stains. Reactions under microwave irradiation were performed on a CEM focused microwave TM synthesis system, Discover-SP W/ ActiVent. NMR spectra were recorded in DMSO- d_6 or CDCl₃ on Bruker (Billerica, MA, USA) instruments DPX 250, AVANCE 300, and AVANCE 500. Tetramethylsilane was used as an internal standard. Chemical shifts (δ) are reported as ppm and coupling constants (J) in Hz. Signal multiplicities are abbreviated as s for singlet, bs for broad singlet, d for doublet, t for triplet, q for quartet, p for pentet, sept for septet, and m for multiplet. Electrospray ionization mass spectrometry (ESI-MS) was performed on a Surveyor MSQ spectrometer (Thermo Fisher), and high-resolution mass spectra (HR-MS) were recorded on a MALDI LTQ Orbitrap XL (Thermo Fisher). The purity of the synthesized compounds **26–31** was determined by high-performance liquid chromatography (HPLC) on a Waters 600 controller HPLC instrument (Waters, Milford, MA, USA) equipped with a Waters 2487 dual absorbance detector, a Waters 717 plus autosampler, and a MultoHigh 100 RP18-5 μm , 240×4 mm column (Phenomenex, Torrance, CA, USA) running a gradient (40% MeOH + 60% H₂O + 0.1% formic acid for 5 min, then for the next 20 min up to only 100% MeOH + 0.1 formic acid and the last 20 min maintained with 100% MeOH + 0.1 formic acid) with a flow rate of 1 mL/min and with UV-detection at $\lambda = 254$ and 280 nm. All compounds used for *in vitro* characterization had a purity $\geq 95\%$ according to HPLC-UV.

1-(Isopropyl(methyl)amino)-3-(naphthalen-1-yloxy)propan-2-ol (26). 2-((Naphthalen-1-yloxy)methyl)oxirane (**34a**, 100 mg, 0.499 mmol, 1.00 equiv) was dissolved in *N*-isopropylmethylamine (**35**, 1.0 mL, 9.6 mmol, 19 equiv) under an inert atmosphere. The reaction mixture was stirred under microwave irradiation at 100 °C for 45 min. After cooling to rt, EtOAc (20 mL) was added, and the mixture was extracted with aqueous HCl solution (1 M, 2 × 15 mL). To the combined aqueous layers, a sodium hydroxide solution (1 M, 35 mL) was added, and the aqueous mixture was extracted with EtOAc (2 × 15 mL). The combined organic layers were washed twice with brine and dried over MgSO₄, and the solvent was removed *in vacuo*. The crude product was purified by silica gel column chromatography (1:1 *n*-hexane/EtOAc + 2% triethylamine) to obtain the title compound as a colorless oil (40 mg, 0.15 mmol, 29%). *R*_f = 0.5 (1:1 *n*-hexane/EtOAc + 2% triethylamine). ¹H NMR (500 MHz, CDCl₃): δ 8.30–8.20 (m, 1H), 7.82–7.78 (m, 1H), 7.51–7.43 (m, 3H), 7.39–7.35 (m, 1H), 6.84 (d, *J* = 7.2 Hz, 1H), 4.27–4.22 (m, 2H), 4.15–4.11 (m, 1H), 3.02 (sept, *J* = 6.6 Hz, 1H), 2.73 (d, *J* = 6.3 Hz, 2H), 2.38 (s, 3H), 1.11 (t, *J* = 7.1 Hz, 6H) ppm. ¹³C NMR (126 MHz, CDCl₃): δ 154.22, 134.65, 127.74, 126.59, 126.01, 125.61, 125.44, 121.79, 120.93, 105.14, 70.17, 65.26, 57.12, 56.28, 37.37, 17.87, 17.14 ppm. MS (ESI+) *m/z*: calcd for C₁₇H₂₄NO₂ ([M + H]⁺), 274.18; found, 274.19. HR-MS (MALDI) *m/z*: calcd for C₁₇H₂₄NO₂ ([M + H]⁺), 274.18016; found, 274.17971.

1-(Naphthalen-1-yloxy)-3-(piperidin-1-yl)propan-2-ol (27). 2-((Naphthalen-1-yloxy)methyl)oxirane (**34a**, 0.10 g, 0.50 mmol, 1.0 equiv) was dissolved in piperidine (**36**, 1.0 mL, 9.6 mmol, 19 equiv) under an inert atmosphere. The reaction mixture was stirred under microwave irradiation at 100 °C for 30 min. After cooling to rt, EtOAc (15 mL) was added, and the mixture was washed with water (3 × 10 mL). The organic layer was dried over MgSO₄, and the solvent was removed *in vacuo* to obtain the title compound as a brown oil (127 mg, 0.445 mmol, 89%). *R*_f = 0.1 (1:1 *n*-hexane/EtOAc). ¹H NMR (500 MHz, CDCl₃): δ 8.28–8.24 (m, 1H), 7.81–7.77 (m, 1H), 7.51–7.45 (m, 2H), 7.44 (d, *J* = 8.3 Hz, 1H), 7.39–7.34 (m, 1H), 6.84 (dd, *J* = 7.5, 0.5 Hz, 1H), 4.33–4.25 (m, 1H), 4.22 (dd, *J* = 9.5, 5.1 Hz, 1H), 4.12 (dd, *J* = 9.5, 5.3 Hz, 1H), 2.77–2.64 (m, 4H), 2.49 (s, 2H), 1.73–1.60 (m, 4H), 1.53–1.45 (m, 2H) ppm. ¹³C NMR (126 MHz, CDCl₃): δ 154.57, 134.64, 127.62, 126.54, 125.97, 125.75, 125.34, 122.08, 120.69, 105.02, 70.73, 65.45, 61.83, 55.00, 25.97, 24.18 ppm. MS (ESI+) *m/z*: calcd for C₁₈H₂₄NO₂ ([M + H]⁺), 286.18; found, 286.19. HR-MS (MALDI) *m/z*: calcd for C₁₈H₂₄NO₂ ([M + H]⁺), 286.18016; found, 286.17968.

1-Isopropoxy-3-(naphthalen-1-yloxy)propan-2-ol (28). A sodium hydride suspension in paraffin oil (60% w/w, 23 mg, 0.32 mmol, 1.3 equiv) was added to 2-propanol (**37**, 5 mL), and the mixture was stirred for 15 min at rt. 2-((Naphthalen-1-yloxy)methyl)oxirane (**34a**, 50 mg, 0.25 mmol, 1.0 equiv) dissolved in 2-propanol (**37**, 2 mL) was added, and the mixture was stirred for 12 h at rt. Aqueous HCl solution (5% v/v, 20 mL) was added, and the mixture was extracted with EtOAc (3 × 15 mL). The combined organic layers were dried over MgSO₄, and the solvent was removed *in vacuo* to obtain the title compound as a yellow oil (59 mg, 0.22 mmol, 90%). *R*_f = 0.2 (4:1 *n*-hexane/EtOAc). ¹H NMR (500 MHz, CDCl₃): δ 8.26–8.23 (m, 1H), 7.83–7.78 (m, 1H), 7.52–7.42 (m, 3H), 7.40–7.33 (m, 1H), 6.85 (d, *J* = 7.1 Hz, 1H), 4.32–4.26 (m, 1H), 4.22 (dd, *J* = 5.5, 2.0 Hz, 2H), 3.75 (dd, *J* = 9.5, 4.4 Hz, 1H), 3.70–3.64 (m, 2H), 1.20 (d, *J* = 2.1 Hz, 3H), 1.19 (d, *J* = 2.1 Hz, 3H) ppm. ¹³C NMR (126 MHz, CDCl₃): δ 154.43, 134.64, 127.68, 126.58, 125.98, 125.70, 125.40, 121.96, 120.78, 105.09, 72.55, 69.49, 69.29, 69.16, 22.23, 22.19 ppm. MS (ESI+) *m/z*: calcd for C₁₆H₂₀O₃Na ([M + Na]⁺), 283.13; found, 283.15. HR-MS (MALDI) *m/z*: calcd for C₁₆H₂₀O₃ ([M]⁺), 260.14070; found, 260.14100.

***N*-Isopropyl-2-methoxy-3-(naphthalen-1-yloxy)propan-1-amine (29).** *tert*-Butylisopropyl(2-methoxy-3-(naphthalen-1-yloxy)propyl)-carbamate (**46**, 38 mg, 0.10 mmol, 1.0 equiv) was dissolved in methylene chloride (5 mL), and a HCl solution in 1,4-dioxane (4 M, 0.44 mL, 1.8 mmol, 18 equiv) was added. The mixture was stirred at rt for 120 h. Aqueous NaOH solution (1 M, 15 mL) was then added, and the mixture was extracted with methylene chloride (3 × 15 mL).

The combined organic layers were dried over Na₂SO₄, and the solvent was evaporated *in vacuo*. The crude product was purified by silica gel column chromatography (4:1 *n*-hexane/EtOAc + 2% triethylamine) to obtain the title compound as a brown solid (25 mg, 0.091 mmol, 90%). *R*_f = 0.3 (4:1 *n*-hexane/EtOAc + 2% triethylamine). ¹H NMR (500 MHz, CDCl₃): δ 8.29–8.18 (m, 1H), 7.81–7.78 (m, 1H), 7.55–7.41 (m, 3H), 7.40–7.32 (m, 1H), 6.82 (d, *J* = 7.4 Hz, 1H), 4.27–4.21 (m, 2H), 3.97–3.90 (m, 1H), 3.59 (s, 3H), 3.04 (dd, *J* = 12.1, 3.8 Hz, 1H), 2.96–2.88 (m, 2H), 1.15 (d, *J* = 3.1 Hz, 3H), 1.14 (d, *J* = 3.1 Hz, 3H) ppm. ¹³C NMR (126 MHz, CDCl₃): δ 154.54, 134.66, 127.64, 126.60, 125.94, 125.75, 125.43, 122.08, 120.75, 104.89, 78.90, 68.66, 58.47, 49.25, 48.67, 22.71, 22.44 ppm. MS (ESI+) *m/z*: calcd for C₁₇H₂₄NO₂ ([M + H]⁺), 274.18; found, 274.25. HR-MS (MALDI) *m/z*: calcd for C₁₇H₂₄NO₂ ([M + H]⁺), 274.18016; found, 274.18114.

***N*-Isopropyl-3-(naphthalen-1-yloxy)propan-1-amine Hydrochloride (30).** 3-(Naphthalen-1-yloxy)propan-1-amine hydrochloride (**41**, 88 mg, 0.37 mmol, 1.0 equiv) was suspended in 1,2-dichloroethane (2 mL) under an inert atmosphere. Triethylamine (100 μL, 0.743 mmol, 2.00 equiv), acetone (**42**, 36 μL, 0.48 mmol, 1.3 equiv), and acetic acid (28 μL, 0.48 mmol, 1.3 equiv) were added, and the suspension was stirred for 30 min at rt. Sodium triacetoxyborohydride (236 mg, 1.11 mmol, 3.00 equiv) was added, and the resulting mixture was stirred at rt for 17 h. Aqueous NaOH solution (2 M, 20 mL) was added, and the mixture was extracted with methylene chloride (1 × 30 mL). The organic layer was washed with water (3 × 10 mL), dried over Na₂SO₄, and concentrated *in vacuo*. The crude product in methylene chloride was treated with a HCl solution in 1,4-dioxane (4 M, 371 μL, 1.49 mmol, 4.00 equiv), and the suspension was stirred for 72 h at rt. The resulting colorless precipitate was filtered off and washed with methylene chloride to obtain the title compound as a colorless solid (48 mg, 0.17 mmol, 46%). *R*_f = 0.5 (9:1 methylene chloride/methanol). ¹H NMR (500 MHz, DMSO-*d*₆): δ 9.04 (s, 2H), 8.23–8.17 (m, 1H), 7.87 (dd, *J* = 7.3, 1.9 Hz, 1H), 7.56–7.46 (m, 3H), 7.45–7.39 (m, 1H), 7.01–6.95 (m, 1H), 4.27 (t, *J* = 6.0 Hz, 2H), 3.38–3.27 (m, 1H), 3.18–3.12 (m, 2H), 2.30–2.24 (m, 2H), 1.28 (d, *J* = 6.5 Hz, 6H) ppm. ¹³C NMR (126 MHz, DMSO-*d*₆): δ 153.74, 134.00, 127.47, 126.45, 126.18, 125.28, 124.84, 121.48, 120.07, 105.23, 65.04, 49.42, 41.36, 25.80, 18.57 ppm. MS (ESI+) *m/z*: calcd for C₁₆H₂₂NO ([M + H]⁺), 244.17; found, 244.05. HR-MS (MALDI) *m/z*: calcd for C₁₆H₂₁NO ([M + H]⁺), 244.16959; found, 244.17072.

1-(Isopropyl(methyl)amino)-3-(quinolin-4-yloxy)propan-2-ol Hydrochloride (31). 4-(Oxiran-2-ylmethoxy)quinoline (**34b**, 571 mg, 2.84 mmol, 1.00 equiv) was dissolved in isopropylamine (**38**, 9.73 mL, 114 mmol, 40.0 equiv). The solution was stirred at 60 °C for 10 h and afterward for 24 h at rt. The excess of isopropylamine was removed *in vacuo*, and the crude product was dissolved in methylene chloride (5 mL). A total of 2.5 mL of this homogenous solution was treated with a HCl solution in 1,4-dioxane (4 M, 2.84 mL, 11.4 mmol, 8.00 equiv). The mixture was stirred at rt for 72 h. The resulting colorless precipitate was filtered off and washed with methanol to obtain the title compound as a colorless solid (366 mg, 1.23 mmol, 87%). *R*_f = 0.5 (9:1 methylene chloride/methanol). ¹H NMR (500 MHz, DMSO-*d*₆): δ 9.26 (s, 1H), 8.86 (s, 1H), 8.56 (d, *J* = 7.3 Hz, 1H), 8.36 (dd, *J* = 8.2, 1.4 Hz, 1H), 8.27 (d, *J* = 8.8 Hz, 1H), 7.98 (ddd, *J* = 8.7, 7.0, 1.5 Hz, 1H), 7.69 (t, *J* = 7.6 Hz, 1H), 6.96 (d, *J* = 7.3 Hz, 1H), 4.94 (dd, *J* = 14.1, 2.6 Hz, 1H), 4.40 (dd, *J* = 14.2, 9.5 Hz, 1H), 4.36–4.28 (m, 1H), 3.37–3.26 (m, 2H), 3.06–2.96 (m, 1H), 1.29 (d, *J* = 4.1 Hz, 3H), 1.28 (d, *J* = 4.1 Hz, 3H) ppm. ¹³C NMR (126 MHz, DMSO-*d*₆): δ 172.49, 148.74, 139.65, 133.70, 126.05, 124.94, 123.37, 118.09, 106.46, 64.77, 56.93, 49.93, 46.76, 18.59, 18.24 ppm. MS (ESI+) *m/z*: calcd for C₁₅H₂₁N₂O₂ ([M + H]⁺), 261.16; found, 261.14. HR-MS (MALDI) *m/z*: calcd for C₁₅H₂₁N₂O₂ ([M + H]⁺), 261.15975; found, 261.16004.

2-((Naphthalen-1-yloxy)methyl)oxirane (34a). *rac*-Epichlorohydrin (**33**, 1.8 mL, 23 mmol, 1.1 equiv) was dissolved in DMF (10 mL). 1-Naphthol (**32a**, 3.00 g, 20.8 mmol, 1.00 equiv) and NaOH (990 mg, 25.1 mmol, 1.20 equiv) were dissolved in a DMF/H₂O (2:1 v/v, 9 mL) mixture and stirred for 50 min at rt. Subsequently, the

alkaline 1-naphthol solution was added dropwise to the previous *rac*-epichlorohydrin solution over 40 min at rt while stirring. After complete addition, the reaction mixture was stirred at rt for 120 h. Water was added, and the mixture was extracted with methylene chloride (3 × 50 mL). The combined organic layers were washed with water and dried over MgSO₄, and the solvent was removed *in vacuo*. The residue was dissolved in 15 mL of EtOAc, and the mixture was washed with water (3 × 15 mL) and dried over MgSO₄, and the solvent was removed *in vacuo*. The crude product was purified by silica gel column chromatography (9:1 *n*-hexane/EtOAc) to obtain the title compound as a purple oil (467 mg, 2.33 mmol, 11%). *R*_f = 0.5 (9:1 *n*-hexane/EtOAc). ¹H NMR (300 MHz, CDCl₃): δ 8.32–8.29 (m, 1H), 7.83–7.78 (m, 1H), 7.53–7.44 (m, 3H), 7.39–7.34 (m, 1H), 6.82 (d, *J* = 7.5 Hz, 1H), 4.41 (dd, *J* = 11.0, 3.2 Hz, 1H), 4.16 (dd, *J* = 10.9, 5.4 Hz, 1H), 3.53–3.48 (m, 1H), 2.99–2.96 (m, 1H), 2.86 (dd, *J* = 4.9, 2.7 Hz, 1H) ppm. ¹³C NMR (75 MHz, CDCl₃): δ 154.40, 134.68, 127.60, 126.65, 125.84, 125.75, 125.47, 122.17, 121.02, 105.15, 69.12, 50.40, 44.92 ppm. MS (MALDI) *m/z*: calcd for C₁₃H₁₂O₂, 200.08; found, 200.08.

4-(Oxiran-2-ylmethoxy)quinoline (34b). Quinoline-4-ol (32b, 1.50 g, 10.3 mmol, 1.00 equiv) was suspended in acetone (10 mL), and a sodium hydride suspension in paraffin oil (60% w/w, 455 mg, 11.4 mmol, 1.10 equiv) was added. The resulting orange solution was stirred at rt for 15 minutes. *rac*-Epichlorohydrin (33, 2.64 mL, 34.1 mmol, 3.30 equiv) was added, and the solution was stirred for 48 h at rt. The solvent was removed *in vacuo*, and the residue was dissolved in methylene chloride (15 mL). The mixture was washed with water (3 × 15 mL); the combined aqueous wash layers were extracted with methylene chloride (3 × 20 mL). The combined organic layers were dried over Na₂SO₄, and the solvent was removed *in vacuo*. The crude product was purified by silica gel column chromatography (19:1 methylene chloride/methanol) to obtain the title compound as a brown oil (571 mg, 2.84 mmol, 27%). *R*_f = 0.6 (9:1 methylene chloride/methanol). ¹H NMR (300 MHz, CDCl₃): δ 8.40 (dd, *J* = 8.1, 1.4 Hz, 1H), 7.63 (ddd, *J* = 8.6, 7.0, 1.6 Hz, 1H), 7.51–7.44 (m, 2H), 7.39–7.29 (m, 1H), 6.21 (d, *J* = 7.8 Hz, 1H), 4.47 (dd, *J* = 15.8, 2.3 Hz, 1H), 4.10 (dd, *J* = 15.8, 5.5 Hz, 1H), 3.35–3.28 (m, 1H), 2.84 (t, *J* = 4.2 Hz, 1H), 2.51 (dd, *J* = 4.4, 2.6 Hz, 1H) ppm. ¹³C NMR (75 MHz, CDCl₃): δ 178.21, 143.59, 140.29, 132.42, 127.16, 127.10, 123.91, 115.36, 110.41, 53.75, 49.89, 45.25 ppm. MS (ESI+) *m/z*: calcd for C₁₂H₁₂NO₂ ([M + H]⁺), 202.09; found, 202.16.

***tert*-Butyl-(3-(naphthalen-1-yloxy)propyl)carbamate (40).** 1-Naphthol (32a, 100 mg, 0.693 mmol, 1.00 equiv) was dissolved in DMF (1 mL) under an inert atmosphere, and a sodium hydride suspension in paraffin oil (60 w/w, 33 mg, 0.83 mmol, 1.2 equiv) was added. The resulting green suspension was stirred at rt for 15 min before *tert*-butyl-(3-bromopropyl)carbamate (39, 198 mg, 0.832 mmol, 1.20 equiv) dissolved in DMF (2 mL) was added. The resulting brown solution was stirred at rt for 24 h. Ethyl acetate (40 mL) was then added, and the mixture was washed with water (5 × 10 mL) and dried over Na₂SO₄, and the solvent was evaporated *in vacuo*. The crude product was purified by silica gel column chromatography (9:1 *n*-hexane/acetone + 2% triethylamine) to obtain the title compound as a colorless solid (185 mg, 0.613 mmol, 88%). *R*_f = 0.3 (9:1 *n*-hexane/acetone + 2% triethylamine). ¹H NMR (300 MHz, CDCl₃): δ 8.30–8.21 (m, 1H), 7.85–7.75 (m, 1H), 7.54–7.32 (m, 4H), 6.81 (dd, *J* = 7.4, 1.0 Hz, 1H), 4.85 (s, 1H), 4.22 (t, *J* = 5.9 Hz, 2H), 3.44 (t, *J* = 6.6 Hz, 2H), 2.13 (p, *J* = 6.3 Hz, 2H), 1.45 (s, 9H) ppm. ¹³C NMR (75 MHz, CDCl₃): δ 156.19, 154.62, 134.65, 127.65, 126.55, 125.98, 125.72, 125.38, 122.02, 120.53, 104.73, 66.26, 38.62, 29.79, 28.56 ppm. MS (ESI+) *m/z*: calcd for C₁₈H₂₃NO₃Na ([M + Na]⁺), 324.16; found, 324.10.

3-(Naphthalen-1-yloxy)propan-1-amine Hydrochloride (41). *tert*-Butyl-(3-(naphthalen-1-yloxy)propyl)carbamate (40, 178 mg, 0.592 mmol, 1.00 equiv) was dissolved in methylene chloride (3 mL), a HCl solution in 1,4-dioxane (4 M, 590 μL, 2.37 mmol, 4.00 equiv) was added, and the solution was stirred at rt for 21 h. The resulting precipitate was filtered off and washed with methylene chloride to obtain the title compound as a colorless solid (113 mg, 0.474 mmol, 80%). *R*_f = 0.4 (4:1 *n*-hexane/acetone + 2% triethylamine). ¹H NMR

(500 MHz, DMSO-*d*₆): δ 8.29–8.08 (m, 4H), 7.91–7.84 (m, 1H), 7.56–7.46 (m, 3H), 7.42 (t, *J* = 7.9 Hz, 1H), 6.97 (d, *J* = 7.5 Hz, 1H), 4.26 (t, *J* = 6.1 Hz, 2H), 3.07 (t, *J* = 7.4 Hz, 2H), 2.23–2.15 (m, 2H) ppm. ¹³C NMR (126 MHz, DMSO-*d*₆): δ 153.75, 134.00, 127.47, 126.45, 126.18, 125.27, 124.86, 121.48, 120.03, 105.22, 64.85, 36.31, 26.91 ppm. MS (ESI+) *m/z*: calcd for C₁₃H₁₆NO ([M + H]⁺), 202.12; found, 201.90. HR-MS (MALDI) *m/z*: calcd for C₁₃H₁₆NO ([M + H]⁺), 202.12264; found, 202.12281.

***tert*-Butyl-(2-hydroxy-3-(naphthalen-1-yloxy)propyl)(isopropyl)carbamate (44).** *rac*-Propranolol hydrochloride (22, 2.00 g, 6.76 mmol, 1.00 equiv), di-*tert*-butyldicarbonate (43, 1.77 g, 8.11 mmol, 1.20 equiv), and NaHCO₃ (1.25 g, 14.9 mmol, 2.20 equiv) were dissolved in H₂O (15 mL). The resulting solution was stirred at rt for 18 h. The mixture was extracted once with EtOAc. The organic layer was dried over MgSO₄, and the solvent was removed *in vacuo* to obtain the title compound as a colorless solid (2.43 g, 6.76 mmol, quant.). *R*_f = 0.7 (1:1 *n*-hexane/EtOAc). ¹H NMR (300 MHz, CDCl₃): δ 8.26–8.20 (m, 1H), 7.84–7.78 (m, 1H), 7.54–7.42 (m, 3H), 7.41–7.34 (m, 1H), 6.85 (dd, *J* = 7.4, 0.9 Hz, 1H), 4.32–4.01 (m, 4H), 3.52 (d, *J* = 4.8 Hz, 2H), 1.51 (s, 9H), 1.24 (d, *J* = 6.9 Hz, 3H), 1.16 (d, *J* = 6.7 Hz, 3H) ppm. ¹³C NMR (75 MHz, CDCl₃): δ 154.31, 134.66, 127.73, 126.54, 126.04, 125.60, 125.38, 121.80, 120.75, 104.94, 80.89, 70.04, 48.81, 47.17, 28.61, 27.56, 21.12, 20.64 ppm. MS (ESI+) *m/z*: calcd for C₂₁H₃₀NO₄ ([M + H]⁺), 360.22; found, 360.41.

***tert*-Butyl-isopropyl(2-methoxy-3-(naphthalen-1-yloxy)propyl)carbamate (46).** *tert*-Butyl-(2-hydroxy-3-(naphthalen-1-yloxy)propyl)(isopropyl)carbamate (44, 400 mg, 1.11 mmol, 1.00 equiv) was dissolved in DMS (45, 1.9 mL, 11 mmol, 10 equiv) and stirred under microwave irradiation at 60 °C for 3 h. After cooling to rt, aqueous NaOH solution (1 M, 20 mL) was added, and the mixture was extracted with EtOAc (3 × 15 mL). The combined organic layers were dried over Na₂SO₄, and the solvent was removed *in vacuo*. The crude product was purified by silica gel column chromatography (9:1 *n*-hexane/EtOAc) to obtain the title compound as a colorless oil (45 mg, 0.12 mmol, 14%). *R*_f = 0.3 (9:1 *n*-hexane/EtOAc). ¹H NMR (300 MHz, CDCl₃): δ 8.31–8.26 (m, 1H), 7.81–7.78 (m, 1H), 7.51–7.45 (m, 2H), 7.43 (d, *J* = 8.2 Hz, 1H), 7.36 (t, *J* = 7.9 Hz, 1H), 6.81 (d, *J* = 7.5 Hz, 1H), 4.30–4.22 (m, 1H), 4.15 (dd, *J* = 10.1, 5.7 Hz, 1H), 3.98 (br s, 1H), 3.58 (s, 3H), 3.54–3.44 (m, 1H), 3.30 (br s, 1H), 1.49 (s, 9H), 1.22 (d, *J* = 6.8 Hz, 3H), 1.18 (d, *J* = 6.8 Hz, 3H) ppm. ¹³C NMR (75 MHz, CDCl₃): δ 154.70, 134.66, 127.59, 126.54, 125.96, 125.81, 125.33, 122.21, 120.59, 104.75, 79.85, 79.35, 69.04, 59.05, 31.58, 29.85, 28.71, 21.07 ppm. MS (ESI+) *m/z*: calcd for C₂₂H₃₁NO₄Na ([M + Na]⁺), 396.22; found, 396.49.

***In Vitro* Methods. Gal4-TLX Reporter Gene Assay.** HEK293T cells were grown in Dulbecco's modified Eagle's medium (DMEM, Thermo Fisher Scientific), high glucose with 10% FCS, sodium pyruvate (1 mM), penicillin (100 U/mL), and streptomycin (100 μg/mL) at 37 °C and 5% CO₂. A period of 24 h before transfection, cells were seeded in 96-well plates (30,000 cells/well) in DMEM with abovementioned supplements. Prior to transfection, medium was changed to Opti-MEM (Thermo Fisher Scientific) without supplements. Cells were then transiently transfected with plasmid mixtures containing pFR-Luc (Stratagene, La Jolla, CA, USA), pRL-SV40 (Promega, Madison, WI, USA), pECE-SV40-Gal4-VP16²¹ (Addgene plasmid 71728, Addgene, Watertown, MA, USA), and pFA-CMV-hTLX-LBD using Lipofectamine LTX reagent (Thermo Fisher Scientific) according to the manufacturer's protocol. Five hours after transfection, cells were treated with Opti-MEM supplemented with penicillin (100 U/mL) and streptomycin (100 μg/mL) additionally containing 0.1% DMSO and the respective test compounds or 0.1% DMSO alone as the negative control. Each sample was tested in duplicates, and every experiment was conducted at least three times. After 14 h of incubation, cells were lysed and assayed for luciferase luminescence using the Dual-Glo luciferase assay system (Promega) according to the manufacturer's protocol. Luminescence was measured with a Tecan Spark M luminometer (Tecan Group AG, Männedorf, Switzerland). To consider transfection efficiency and cell growth, the obtained firefly luciferase signal

was normalized by dividing firefly luciferase signals by *Renilla* luciferase signals and multiplying by a factor of 1000 to obtain relative light units (RLU). Fold reporter activation or repression was obtained by dividing the mean RLU of a test compound at a respective concentration by the mean RLU of the 0.1% DMSO control. IC₅₀ and EC₅₀ values were obtained by plotting fold reporter activation versus test compound concentrations and fitting the resulting sigmoidal curve with a four-parameter logistic regression in SigmaPlot 12.5. Separate control experiments to exclude nonspecific cellular or VP16-mediated effects were performed following the same procedure with the exception that cells were only transfected with pFR-Luc, pRL-SV40, and pECE-SV40-Gal4-VP16.

Gal4-NR Reporter Gene Assays for Selectivity Profiling. Selectivity profiling was performed in hybrid reporter gene assays in HEK293T cells transiently transfected (as described for Gal4-TLX) with plasmids encoding the respective Gal4-NR hybrid receptor, pRL-SV40, and pFR-Luc. The following Gal4-NR plasmids and reference agonists (at 1 μ M) were used: pFA-CMV-hCAR-LBD (CITCO),³³ pFA-CMV-hFXR-LBD (GW4064),³⁴ pFA-CMV-hLXR α -LBD (T0901317),³⁴ pFA-CMV-hLXR β -LBD (T0901317),³⁴ pFA-CMV-hPPAR α -LBD (GW7647),³⁵ pFA-CMV-hPPAR γ -LBD (pioglitazone),³⁵ pFA-CMV-hPPAR δ -LBD (L165041),³⁵ pFA-CMV-hRAR α -LBD (tretinoin),³³ pFA-CMV-hRXR α -LBD (bexarotene),³³ pFA-CMV-hTHR α -LBD (T3),³⁶ and pFA-CMV-hVDR-LBD (calcitriol).³³

Full-Length TLX/TAE Reporter Gene Assay. The full-length TLX reporter gene assay was performed in transiently transfected HEK293T cells (as described for Gal4-TLX) using pFA-CMV-hTLX encoding hTLX, pFR-TAE-Luc encoding firefly luciferase under the control of the TLX-activating element (TAE) from the SIRT1 promoter region, and pRL-SV40. pFA-CMV-hTLX full length was obtained by inserting the TLX coding sequence (CDS) into pFA-CMV (Agilent Technologies) while replacing the CDS for Gal4. For this purpose, the vector backbone was amplified by polymerase chain reaction (PCR) using high-fidelity DNA polymerase Q5 (New England Biolabs) with primers KpnI.f: CCC CGG TAC CAG ATC TTG AAT AAG TAG and BamHI.r: GCT TGG ATC CCA TGA TTC AGG AGG CTT GCT TAT CG. This resulted in a BamHI cleavage site positioned immediately after the start-Met of the former Gal4 CDS. A complementary DNA (cDNA) fragment obtained from PCR amplification using the natural cDNA (TLX BC028031.1, purchased as IMAGE cDNA clone #5242079 from Source BioScience, Nottingham, UK) was cloned between the newly introduced BamHI cleavage site and the KpnI site of the original multiple cloning site. The TLX open reading frame encodes Met-Gly-(NR2E1; uniprot entry: Q9Y466-1 residues 2–385). pFR-TAE-Luc was cloned based on the reporter plasmid pFR-Luc (Stratagene) used for the Gal4-hybrid assays, which contains a section between 178–83 bp upstream of the start codon of the firefly CDS that encompasses five copies of the Gal4 response element. For the transactivation assay based on full-length TLX, this section was replaced with the sequence GGTACCGGGT**TCACGTGACGGG**GAGCTC to obtain pFR-TAE-Luc. The minimal TLX-activating element is preceded by GGG and flanked by restriction sites for KpnI and SacI in order to resemble construct #10 reported by Iwahara *et al.*⁷

Expression of Recombinant TLX-LBD Protein. The recombinant TLX-LBD with an N-terminal His₆-tag was expressed in *Escherichia coli* Rosetta. Cells were initially cultured in TB medium at 37 °C to an OD₆₀₀ of 2.8 prior to induction with 0.5 mM isopropyl β -D-1-thiogalactopyranoside at 18 °C overnight. Cells were harvested and resuspended in a buffer containing 50 mM N-(2-hydroxyethyl)-piperazine-N'-ethanesulfonic acid (HEPES), pH 7.5, 500 mM NaCl, 20 mM imidazole, 5% glycerol, and 1 mM TCEP and lysed by sonication. The recombinant TLX-LBD protein was initially purified by Ni²⁺ affinity chromatography. The histidine tag was removed by TEV protease treatment, and the cleaved protein was separated by reverse Ni²⁺ affinity purification. The protein was further purified by size exclusion chromatography and stored in 20 mM Tris, pH 7.5, 150 mM NaCl, 0.2 mM TCEP, and 5% glycerol.

Differential Scanning Fluorimetry. Experiments were conducted on an Mx3005p real-time PCR machine (Stratagene, San Diego, CA, USA) following a published protocol.³⁷ A total of 2 μ M recombinant TLX-LBD protein in buffer (10 mM HEPES pH 7.5; 100 mM NaCl) supplemented with SYPRO Orange dye (1:1000 dilution) was tested with **2**, **4**, **5**, **7–13**, **16**, and **18–20** at a final concentration of 500 μ M with an untreated control (5% DMSO) in 71 cycles (1 °C/cycle). Dydrogesterone and ccrp2 served as reference TLX ligands and caused a comparable thermal shift (ΔT_m) as reported previously.¹⁷ Each compound was tested in three independent experiments. Amplification plots were analyzed using a Boltzmann fit to obtain melting points (T_m). ΔT_m corresponds to $\Delta T_m = T_m$ (compound) – T_m (untreated).

Isothermal Titration Calorimetry. ITC was conducted on an Affinity ITC instrument (TA Instruments, New Castle, DE, USA). Experiments were performed at 25 °C, and the stirring rate was set to 75 rpm. A total of 40 μ M TLX-LBD protein in buffer containing 1% DMSO (20 mM Tris, pH 7.5, 150 mM NaCl, 0.2 mM TCEP, and 5% glycerol) was titrated with **22** (200 μ M in the same buffer containing 1% DMSO, 31 injections: 1 \times 1 μ L and 30 \times 3 μ L). The injection interval was set to 300 s. As control experiments, **22** (200 μ M) was titrated into buffer, and the buffer was titrated to the TLX-LBD protein under otherwise identical conditions. The heat rates of the **22**–TLX-LBD titration were corrected by subtracting the **22**–buffer experiment to obtain corrected heat rates, which were analyzed using an independent binding model using NanoAnalyze software (TA Instruments, New Castle, DE, USA).

Quantification of TLX-Regulated Gene Expression in T98G Cells. T98G cells (Sigma-Aldrich) were cultured in DMEM (Thermo Fisher Scientific), high glucose supplemented with 10% FCS, sodium pyruvate (1 mM), penicillin (100 U/mL), and streptomycin (100 μ g/mL) at 37 °C and 5% CO₂. For gene expression experiments, cells were seeded in 6-well plates (1 \times 10⁶ cells/well). A period of 24 h after seeding, medium was changed to minimal essential medium (MEM) supplemented with 1% charcoal-stripped FCS, penicillin (100 U/mL), streptomycin (100 μ g/mL), and L-glutamine (2 mM). After 24 h, T98G cells were incubated with the test compounds [propranolol (**22**, 50 μ M) and atenolol (**24**, 50 μ M)] dissolved in the same medium additionally containing 0.1% DMSO or 0.1% DMSO alone as an untreated control for 8 h. Cells were then harvested, washed with cold phosphate-buffered saline (PBS), and used directly for mRNA extraction using the E.Z.N.A. total RNA kit I (R6834-02, Omega Bio-Tek, Inc., Norcross, GA, USA). Extracted mRNA was reverse-transcribed into cDNA using the high-capacity RNA-to-cDNA kit (cat #4387406, Thermo Fischer Scientific, Inc.). TLX-regulated gene expression was analyzed by quantitative real-time PCR on a StepOnePlus system (Life Technologies, Carlsbad, CA, USA) using Power SYBR Green (Life Technologies). Each sample was analyzed in duplicates, repeating in at least four independent experiments. Data were analyzed by the comparative $\Delta\Delta C_T$ method with glyceraldehyde 3-phosphate dehydrogenase (GAPDH) as a reference gene. The following primers (for the human genes) were used: GAPDH:³⁸ forward 5'-CCT GTT CGA CAG TCA GCC G-3', reverse 5'-CGA CCA AAT CCG TTG ACT CC-3'; SIRT1:⁷ forward 5'-GAA CCT TTG CCT CAT CTA CA-3', reverse 5'-AGC CGC TTA CTA ATC TGC TC-3'; TET3:²⁸ forward 5'-CAG CAG CCG AGA AGA AGA AG-3', reverse 5'-GGA CAA TCC ACC CTT CAG AG-3'; PTEN (Origene, Rockville, MD, USA): forward 5'-TGA GTT CCC TCA GCC GTT ACC T-3', reverse 5'-GAG GTT TCC TCT GGT CCT GGT A-3'; TLX:⁷ forward 5'-CTA AGA GTG TGC CAG CCT TC-3', reverse 5'-TGT TAG CAT CAA CCG GAA TGG-3'.

Directed Migration (Boyden Chamber Assay). To analyze potential effects of propranolol (**22**) on the directed migration of the glioblastoma cell line T98G in the direction of a serum gradient, a Boyden chamber assay was performed. A total of 150,000 T98G cells were seeded on Transwell inserts (growth area 0.33 cm², 8 μ m pore size, polycarbonate, Corning, NY, USA) and were treated with propranolol (**22**, 75 μ M), the β adrenoceptor antagonists atenolol (**24**) or sotalol (**25**), the inactive control substance **31** (75 μ M), or

vehicle (DMSO 0.1%; Sigma-Aldrich, St. Louis, MO, USA) in serum-free DMEM (Thermo Fisher Scientific) supplemented with sodium pyruvate (1 mM), penicillin (100 U/mL), and streptomycin (100 μ g/mL). For the generation of a serum gradient, 10% FCS was added to the lower compartment of the insert for the compound treatment groups and for the positive control. For the negative control, serum-free DMEM was added into the lower chamber. The cells were allowed to migrate in the direction of the serum gradient for 24 h before they were fixed with a methanol–ethanol solution (ratio 2:1) for 10 min. Subsequently, the cells were stained using a methanolic (20%) crystal violet solution (Sigma-Aldrich, St. Louis, MO, USA) for 20 min. Non-migrated cells were removed from the upper part of the Transwell insert membrane using a cotton swab. After air drying overnight, 20% acetic acid was used to resolve DNA-bound crystal violet. Cell-leached crystal violet was quantified by absorption measurement at 590 nm using a plate reader (SPECTRAFluor Plus; Tecan). The data were quantified using GraphPad Prism version 5.0 (San Diego, USA), and statistical significance was ascertained deploying one-way analysis of variance (ANOVA) followed by Tukey's *post hoc* test. Data are expressed as mean \pm SEM and considered as statistically significant when $p \leq 0.05$.

Proliferation Assay. Potential effects of propranolol on proliferation of T98G cells were determined by crystal violet staining. A total of 4000 cells per well of a 96-well plate (Greiner Bio-One, Frickenhausen, Germany) were seeded in DMEM supplemented with 10% FCS, sodium pyruvate (1 mM), penicillin (100 U/mL), and streptomycin (100 μ g/mL). After 24 h, the cells were treated with indicated concentrations of propranolol (**22**), the β adrenoceptor antagonists atenolol (**24**) or sotalol (**25**), the control compound **31**, or vehicle (DMSO 0.1%). Additionally, untreated cells were fixed using a methanol–ethanol solution (ratio 2:1) for 10 min. Compound- and vehicle-treated T98G cells were allowed to proliferate for 72 h before they were fixed and stained with crystal violet together with control cells. After air drying overnight, DNA-bound crystal violet was resolved using 20% acetic acid. The cell number was determined by absorption measurement at 590 nm using a plate reader (SPECTRAFluor Plus; Tecan). For quantification of cell proliferation, the absorption values of control cells were subtracted from compound- and vehicle-treated T98G cells. In addition, 4000 cells per well of a 96-well plate were treated 24 h post seeding with indicated concentrations of propranolol (**22**), the β adrenoceptor antagonists atenolol (**24**) or sotalol (**25**), **31**, or vehicle (0.1% DMSO). After 72 h, WST reagent (Sigma-Aldrich) was added to the cells and incubated for 30 min before absorption was measured on a plate reader (Varioskan Flash, Thermo Fisher Scientific, Dreieich, Germany) at 450 and 620 nm for reference. The data were quantified using GraphPad Prism version 5.0 (San Diego, USA), and statistical significance was ascertained deploying one-way ANOVA followed by Tukey's *post hoc* test. Data are expressed as mean \pm SEM and considered as statistically significant when $p \leq 0.05$. IC₅₀ values were calculated using asymmetrical (five-parameter) dose–response curves.

Apoptosis Assay. To exclude potential compound-derived effects on cell death, an apoptosis assay according to Nicoletti *et al.*³² was performed. In brief, 24,000 T98G cells were seeded on 24-well plates (Greiner Bio-One). After 24 h, the cells were treated with indicated concentrations of propranolol (**22**), **24**, **25**, **31**, or the vehicle (DMSO 0.1%). After 72 h of incubation T98G cells were detached by trypsinization. In addition, 24 h before the end of the incubation period, apoptosis was induced in control cells using staurosporine (1 μ M; Sigma-Aldrich). All solutions including washing solutions were collected in reaction tubes and centrifuged at 300g for 5 min at 4 °C. After washing with ice-cold PBS and an additional centrifugation step, the cells were incubated overnight with a PI (50 μ g/mL; Sigma-Aldrich) solution containing 0.1% sodium citrate and 0.1% Triton-X 100. Apoptotic cells were determined by flow cytometry (FACSVerse; BD Biosciences, San Jose, CA, USA). The data were quantified using GraphPad Prism version 5.0 (San Diego, USA), and statistical significance was ascertained deploying one-way ANOVA followed by

Tukey's *post hoc* test. Data are expressed as mean \pm SEM and considered as statistically significant when $p \leq 0.05$.

Analysis of Cell Membrane Integrity. For the exclusion of potential compound-derived effects on cell membrane integrity, an assay measuring LDH activity in cell culture supernatants was performed according to the manufacturer's instructions (CytoTox 96 Non-Radioactive Cytotoxicity Assay; Promega Heidelberg, Germany). A total of 4000 T98G cells per well were seeded on 96-well plates. After 24 h, the cells were treated with indicated concentrations of propranolol (**22**), **24**, **25**, **31** or, the vehicle (DMSO 0.1%). Control cells were treated with a lysis solution from the kit 45 min before the end of the incubation period of 72 h. Subsequently, 50 μ L of cell culture supernatants was transferred into a new plate, and a substrate solution was added (50 μ L). After 30 min, the enzymatic reaction was terminated by the addition of stopping solution (50 μ L), and absorption was measured at 490 nm using a plate reader (Varioskan Flash). The data were quantified using GraphPad Prism version 5.0 (San Diego, USA), and statistical significance was ascertained deploying one-way ANOVA followed by Tukey's *post hoc* test. Data are expressed as mean \pm SEM and considered as statistically significant when $p \leq 0.05$.

■ ASSOCIATED CONTENT

Supporting Information

The Supporting Information is available free of charge at <https://pubs.acs.org/doi/10.1021/acs.jmedchem.1c00733>.

Supporting figures and tables and HPLC traces for compounds **26–31** (PDF)

Molecular formula strings containing structures and activity data (CSV)

■ AUTHOR INFORMATION

Corresponding Author

Daniel Merk – Institute of Pharmaceutical Chemistry, Goethe University Frankfurt, 60438 Frankfurt, Germany;

orcid.org/0000-0002-5359-8128; Email: merk@pharmchem.uni-frankfurt.de

Authors

Giuseppe Faudone – Institute of Pharmaceutical Chemistry, Goethe University Frankfurt, 60438 Frankfurt, Germany

Iris Bischoff-Kont – Institute of Pharmaceutical Biology, Goethe University Frankfurt, 60438 Frankfurt, Germany

Lea Racher – Institute of Pharmaceutical Chemistry, Goethe University Frankfurt, 60438 Frankfurt, Germany

Sabine Willems – Institute of Pharmaceutical Chemistry, Goethe University Frankfurt, 60438 Frankfurt, Germany

Rezart Zhubi – Institute of Pharmaceutical Chemistry, Goethe University Frankfurt, 60438 Frankfurt, Germany; Structural Genomics Consortium, BMLS, Goethe University Frankfurt, 60438 Frankfurt, Germany

Astrid Kaiser – Institute of Pharmaceutical Chemistry, Goethe University Frankfurt, 60438 Frankfurt, Germany

Apirat Chaikwad – Institute of Pharmaceutical Chemistry, Goethe University Frankfurt, 60438 Frankfurt, Germany; Structural Genomics Consortium, BMLS, Goethe University Frankfurt, 60438 Frankfurt, Germany; orcid.org/0000-0003-1120-2209

Stefan Knapp – Institute of Pharmaceutical Chemistry, Goethe University Frankfurt, 60438 Frankfurt, Germany; Structural Genomics Consortium, BMLS, Goethe University Frankfurt, 60438 Frankfurt, Germany; orcid.org/0000-0001-5995-6494

Robert Fürst – Institute of Pharmaceutical Biology, Goethe University Frankfurt, 60438 Frankfurt, Germany

Jan Heering – Fraunhofer Institute for Translational Medicine and Pharmacology ITMP, 60596 Frankfurt, Germany;
orcid.org/0000-0002-4922-1993

Complete contact information is available at:
<https://pubs.acs.org/10.1021/acs.jmedchem.1c00733>

Author Contributions

All authors have given approval to the final version of the manuscript.

Notes

The authors declare no competing financial interest.

ACKNOWLEDGMENTS

This research was financially supported by the Aventis Foundation (Life Science Bridge Award to D.M.). Gal4-VP16 was a gift from Lea Sistonen (Addgene plasmid #71728). The authors thank Isabell Franz for support.

ABBREVIATIONS

FCS, fetal calf serum; LBD, ligand-binding domain; LDH, lactate dehydrogenase; NSC, neural stem cells; PAINS, pan-assay interference substances; PTEN, phosphatase and tensin homologue; SAR, structure–activity relationship; SIRT1, sirtuin 1; stps, staurosporin; TET3, Tet methylcytosine dioxygenase 3; TLX, tailless homologue receptor

REFERENCES

- (1) Shi, Y.; Chichung Lie, D.; Taupin, P.; Nakashima, K.; Ray, J.; Yu, R. T.; Gage, F. H.; Evans, R. M. Expression and Function of Orphan Nuclear Receptor TLX in Adult Neural Stem Cells. *Nature* **2004**, *427*, 78–83.
- (2) Miyawaki, T. Tlx, an Orphan Nuclear Receptor, Regulates Cell Numbers and Astrocyte Development in the Developing Retina. *J. Neurosci.* **2004**, *24*, 8124–8134.
- (3) Sun, G.; Yu, R. T.; Evans, R. M.; Shi, Y. Orphan Nuclear Receptor TLX Recruits Histone Deacetylases to Repress Transcription and Regulate Neural Stem Cell Proliferation. *Proc. Natl. Acad. Sci. U.S.A.* **2007**, *104*, 15282–15287.
- (4) Yokoyama, A.; Takezawa, S.; Schüle, R.; Kitagawa, H.; Kato, S. Transrepressive Function of TLX Requires the Histone Demethylase LSD1. *Mol. Cell. Biol.* **2008**, *28*, 3995–4003.
- (5) Zhang, C.-L.; Zou, Y.; Yu, R. T.; Gage, F. H.; Evans, R. M. Nuclear Receptor TLX Prevents Retinal Dystrophy and Recruits the Corepressor Atrophin1. *Genes Dev.* **2006**, *20*, 1308–1320.
- (6) Estruch, S. B.; Buzón, V.; Carbó, L. R.; Schorova, L.; Lüders, J.; Estébanez-Perpiñá, E. The Oncoprotein BCL11A Binds to Orphan Nuclear Receptor TLX and Potentiates Its Transrepressive Function. *PLoS One* **2012**, *7*, No. e37963.
- (7) Iwahara, N.; Hisahara, S.; Hayashi, T.; Horio, Y. Transcriptional Activation of NAD⁺-Dependent Protein Deacetylase SIRT1 by Nuclear Receptor TLX. *Biochem. Biophys. Res. Commun.* **2009**, *386*, 671–675.
- (8) Liu, H.-K.; Belz, T.; Bock, D.; Takacs, A.; Wu, H.; Lichter, P.; Chai, M.; Schütz, G. The Nuclear Receptor Tailless Is Required for Neurogenesis in the Adult Subventricular Zone. *Genes Dev.* **2008**, *22*, 2473–2478.
- (9) Abrahams, B. S.; Kwok, M. C. H.; Trinh, E.; Budaghzadeh, S.; Hossain, S. M.; Simpson, E. M. Pathological Aggression in “Fierce” Mice Corrected by Human Nuclear Receptor 2E1. *J. Neurosci.* **2005**, *25*, 6263–6270.
- (10) Davis, S. M.; Thomas, A. L.; Nomie, K. J.; Huang, L.; Dierick, H. A. Tailless and Atrophin Control Drosophila Aggression by Regulating Neuropeptide Signalling in the Pars Intercerebralis. *Nat. Commun.* **2014**, *5*, 3177.

(11) Kumar, R. A.; McGhee, K. A.; Leach, S.; Bonaguro, R.; Maclean, A.; Aguirre-Hernandez, R.; Abrahams, B. S.; Coccaro, E. F.; Hodgins, S.; Turecki, G.; Condon, A.; Muir, W. J.; Brooks-Wilson, A. R.; Blackwood, D. H.; Simpson, E. M. Initial Association of NR2E1 with Bipolar Disorder and Identification of Candidate Mutations in Bipolar Disorder, Schizophrenia, and Aggression through Resequencing. *Am. J. Med. Genet., Part B* **2008**, *147*, 880–889.

(12) O’Leary, J. D.; Kozareva, D. A.; Hueston, C. M.; O’Leary, O. F.; Cryan, J. F.; Nolan, Y. M. The Nuclear Receptor Tlx Regulates Motor, Cognitive and Anxiety-Related Behaviours during Adolescence and Adulthood. *Behav. Brain Res.* **2016**, *306*, 36–47.

(13) Kozareva, D. A.; O’Leary, O. F.; Cryan, J. F.; Nolan, Y. M. Deletion of TLX and Social Isolation Impairs Exercise-Induced Neurogenesis in the Adolescent Hippocampus. *Hippocampus* **2018**, *28*, 3–11.

(14) O’Leary, J. D.; O’Leary, O. F.; Cryan, J. F.; Nolan, Y. M. Regulation of Behaviour by the Nuclear Receptor TLX. *Genes, Brain Behav.* **2018**, *17*, No. e12357.

(15) Zou, Y.; Niu, W.; Qin, S.; Downes, M.; Burns, D. K.; Zhang, C.-L. The Nuclear Receptor TLX Is Required for Gliomagenesis within the Adult Neurogenic Niche. *Mol. Cell. Biol.* **2012**, *32*, 4811–4820.

(16) Chavali, P. L.; Saini, R. K. R.; Zhai, Q.; Vizlin-Hodzic, D.; Venkatabalasubramanian, S.; Hayashi, A.; Johansson, E.; Zeng, Z.-j.; Mohlin, S.; Pählman, S.; Hansford, L.; Kaplan, D. R.; Funari, K. TLX Activates MMP-2, Promotes Self-Renewal of Tumor Spheres in Neuroblastoma and Correlates with Poor Patient Survival. *Cell Death Dis.* **2014**, *5*, No. e1502.

(17) Benod, C.; Villagomez, R.; Filgueira, C. S.; Hwang, P. K.; Leonard, P. G.; Poncet-Montange, G.; Rajagopalan, S.; Fletterick, R. J.; Gustafsson, J.-Å.; Webb, P. The Human Orphan Nuclear Receptor Tailless (TLX, NR2E1) Is Druggable. *PLoS One* **2014**, *9*, No. e99440.

(18) Dueva, E.; Singh, K.; Kalyta, A.; LeBlanc, E.; Rennie, P.; Cherkasov, A. Computer-aided discovery of small molecule inhibitors of transcriptional activity of TLX (NR2E1) nuclear receptor. *Molecules* **2018**, *23*, 2967.

(19) Griffett, K.; Bedia-Diaz, G.; Hegazy, L.; de Vera, I. M. S.; Wanninayake, U. S.; Billon, C.; Koelblen, T.; Wilhelm, M. L.; Burris, T. P. The Orphan Nuclear Receptor TLX Is a Receptor for Synthetic and Natural Retinoids. *Cell Chem. Biol.* **2020**, *27*, 1272–1284.

(20) Heering, J.; Merk, D. Hybrid Reporter Gene Assays: Versatile In Vitro Tools to Characterize Nuclear Receptor Modulators. In *Methods in Molecular Biology*; Badr, M., Ed.; Humana, 2019; Vol. 1966, pp 175–192.

(21) Budzyński, M. A.; Puustinen, M. C.; Joutsen, J.; Sistonen, L. Uncoupling Stress-Inducible Phosphorylation of Heat Shock Factor 1 from Its Activation. *Mol. Cell. Biol.* **2015**, *35*, 2530–2540.

(22) Sadowski, I.; Ma, J.; Triezenberg, S.; Ptashne, M. GAL4-VP16 Is an Unusually Potent Transcriptional Activator. *Nature* **1988**, *335*, 563–564.

(23) Meijer, I.; Willems, S.; Ni, X.; Heering, J.; Chaikwad, A.; Merk, D. Chemical Starting Matter for HNF4 α Ligand Discovery and Chemogenomics. *Int. J. Mol. Sci.* **2020**, *21*, 7895.

(24) De Bosscher, K.; Desmet, S. J.; Clarisse, D.; Estébanez-Perpiñá, E.; Brunsveld, L. Nuclear Receptor Crosstalk—Defining the Mechanisms for Therapeutic Innovation. *Nat. Rev. Endocrinol.* **2020**, *16*, 363–377.

(25) Yoo, Y.-G.; Na, T.-Y.; Yang, W.-K.; Kim, H.-J.; Lee, I.-K.; Kong, G.; Chung, J.-H.; Lee, M.-O. 6-Mercaptopurine, an Activator of Nur77, Enhances Transcriptional Activity of HIF-1 α Resulting in New Vessel Formation. *Oncogene* **2007**, *26*, 3823–3834.

(26) Wansa, K. D. S. A.; Harris, J. M.; Yan, G.; Ordentlich, P.; Muscat, G. E. O. The AF-1 Domain of the Orphan Nuclear Receptor NOR-1 Mediates Trans-Activation, Coactivator Recruitment, and Activation by the Purine Anti-Metabolite 6-Mercaptopurine. *J. Biol. Chem.* **2003**, *278*, 24776–24790.

(27) Wishart, D. S.; Feunang, Y. D.; Guo, A. C.; Lo, E. J.; Marcu, A.; Grant, J. R.; Sajed, T.; Johnson, D.; Li, C.; Sayeeda, Z.; Assempour, N.; Iynkkaran, I.; Liu, Y.; MacIejewski, A.; Gale, N.; Wilson, A.; Chin, L.; Cummings, R.; Le, D.; Pon, A.; Knox, C.; Wilson, M. DrugBank

5.0: A Major Update to the DrugBank Database for 2018. *Nucleic Acids Res.* **2018**, *46*, D1074–D1082.

(28) Cui, Q.; Yang, S.; Ye, P.; Tian, E.; Sun, G.; Zhou, J.; Sun, G.; Liu, X.; Chen, C.; Murai, K.; Zhao, C.; Azizian, K. T.; Yang, L.; Warden, C.; Wu, X.; D'Apuzzo, M.; Brown, C.; Badie, B.; Peng, L.; Riggs, A. D.; Rossi, J. J.; Shi, Y. Downregulation of TLX Induces TET3 Expression and Inhibits Glioblastoma Stem Cell Self-Renewal and Tumorigenesis. *Nat. Commun.* **2016**, *7*, 10637.

(29) Biryán, F.; Demirelli, K.; Torğut, G.; Pihtili, G. Synthesis, Thermal Degradation and Dielectric Properties of Poly[2-Hydroxy,3-(1-Naphthoxy)Propyl Methacrylate]. *Polym. Bull.* **2017**, *74*, 583–602.

(30) Abdel-Magid, A. F.; Carson, K. G.; Harris, B. D.; Maryanoff, C. A.; Shah, R. D. Reductive Amination of Aldehydes and Ketones with Sodium Triacetoxyborohydride. Studies on Direct and Indirect Reductive Amination Procedures. *J. Org. Chem.* **1996**, *61*, 3849–3862.

(31) Abdel-Magid, A. F.; Mehrman, S. J. A Review on the Use of Sodium Triacetoxyborohydride in the Reductive Amination of Ketones and Aldehydes. *Org. Process Res. Dev.* **2006**, *10*, 971–1031.

(32) Nicoletti, I.; Migliorati, G.; Pagliacci, M. C.; Grignani, F.; Riccardi, C. A Rapid and Simple Method for Measuring Thymocyte Apoptosis by Propidium Iodide Staining and Flow Cytometry. *J. Immunol. Methods* **1991**, *139*, 271–279.

(33) Flesch, D.; Cheung, S.-Y.; Schmidt, J.; Gabler, M.; Heitel, P.; Kramer, J.; Kaiser, A.; Hartmann, M.; Lindner, M.; Lüddens-Dämgen, K.; Heering, J.; Lamers, C.; Lüddens, H.; Wurglics, M.; Proschak, E.; Schubert-Zsilavecz, M.; Merk, D. Non-Acidic Farnesoid X Receptor Modulators. *J. Med. Chem.* **2017**, *60*, 7199–7205.

(34) Heitel, P.; Achenbach, J.; Moser, D.; Proschak, E.; Merk, D. DrugBank Screening Revealed Alitretinoin and Bexarotene as Liver X Receptor Modulators. *Bioorg. Med. Chem. Lett.* **2017**, *27*, 1193–1198.

(35) Rau, O.; Wurglics, M.; Paulke, A.; Zitzkowski, J.; Meindl, N.; Bock, A.; Dingermann, T.; Abdel-Tawab, M.; Schubert-Zsilavecz, M. Carnosic Acid and Carnosol, Phenolic Diterpene Compounds of the Labiate Herbs Rosemary and Sage, Are Activators of the Human Peroxisome Proliferator-Activated Receptor Gamma. *Planta Med.* **2006**, *72*, 881–887.

(36) Gellrich, L.; Heitel, P.; Heering, J.; Kilu, W.; Pollinger, J.; Goebel, T.; Kahnt, A.; Arifi, S.; Pogoda, W.; Paulke, A.; Steinhilber, D.; Proschak, E.; Wurglics, M.; Schubert-Zsilavecz, M.; Chaikuad, A.; Knapp, S.; Bischoff, I.; Fürst, R.; Merk, D. L-Thyroxin and the Nonclassical Thyroid Hormone TETRAC Are Potent Activators of PPAR γ . *J. Med. Chem.* **2020**, *63*, 6727–6740.

(37) Niesen, F. H.; Berglund, H.; Vedadi, M. The Use of Differential Scanning Fluorimetry to Detect Ligand Interactions That Promote Protein Stability. *Nat. Protoc.* **2007**, *2*, 2212–2221.

(38) Schmidt, J.; Klingler, F.-M.; Proschak, E.; Steinhilber, D.; Schubert-Zsilavecz, M.; Merk, D. NSAIDs Ibuprofen, Indometacin, and Diclofenac Do Not Interact with Farnesoid X Receptor. *Sci. Rep.* **2015**, *5*, 14782.